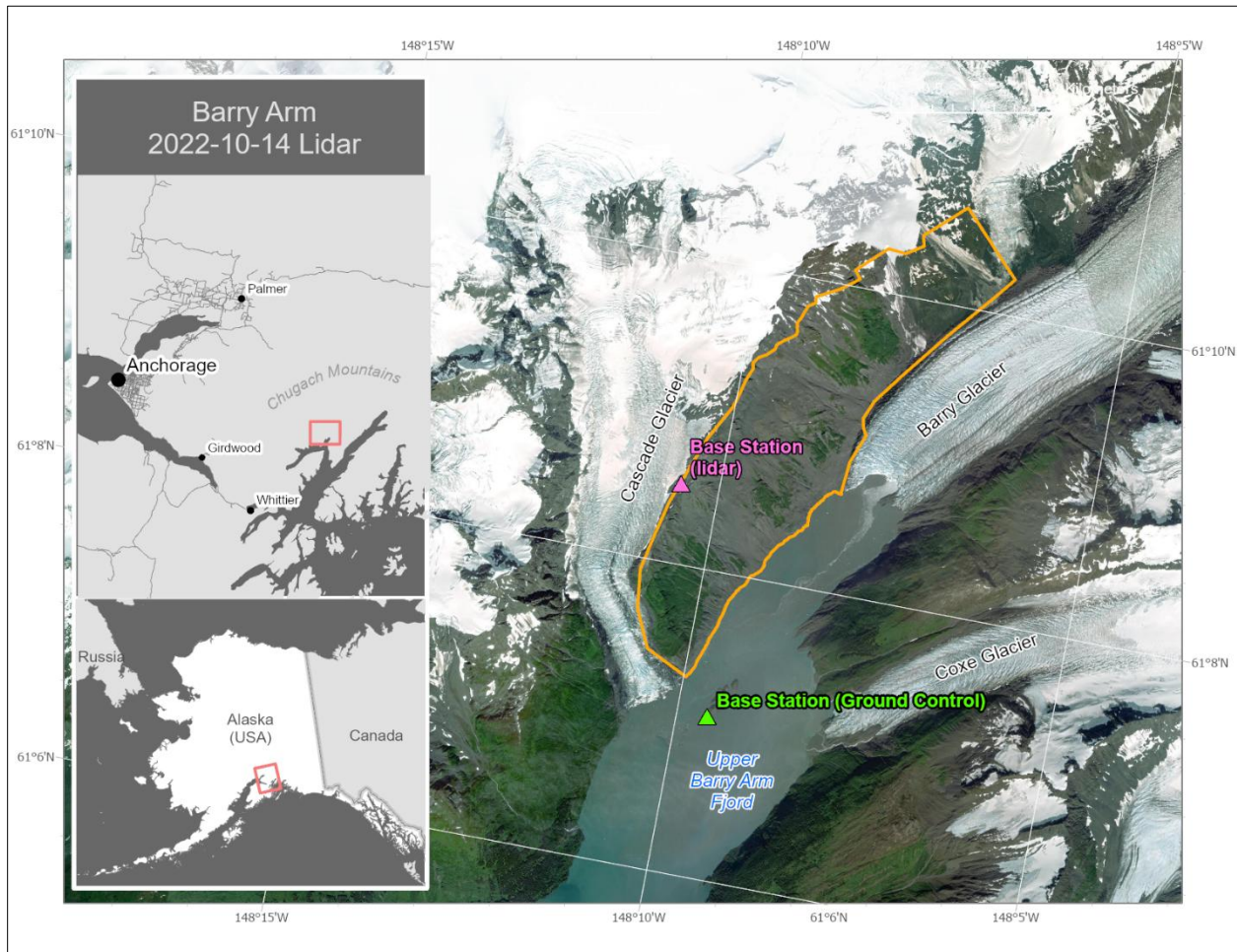


LIDAR-DERIVED ELEVATION DATA FOR UPPER BARRY ARM FJORD, SOUTHCENTRAL ALASKA, COLLECTED OCTOBER 14, 2022

Katreen M. Wikstrom Jones, Gabriel J. Wolken, and Ronald P. Daanen

Raw Data File 2026-10



Location map of the survey area with an orthometric image.

This report has not been reviewed for technical content or for conformity to the editorial standards of DGGS

2026
STATE OF ALASKA
DEPARTMENT OF NATURAL RESOURCES
DIVISION OF GEOLOGICAL & GEOPHYSICAL SURVEYS



STATE OF ALASKA

Mike Dunleavy, Governor

DEPARTMENT OF NATURAL RESOURCES

John Crowther, Commissioner-Designee

DIVISION OF GEOLOGICAL & GEOPHYSICAL SURVEYS

Erin A. Campbell, State Geologist & Director

Publications produced by the Division of Geological & Geophysical Surveys are available to download from the DGGS website (dgg.alaska.gov). Publications on hard-copy or digital media can be examined or purchased in the Fairbanks office:

Alaska Division of Geological & Geophysical Surveys (DGGS)

3354 College Road | Fairbanks, Alaska 99709-3707

Phone: 907.451.5010 | Fax 907.451.5050

dggspubs@alaska.gov | dgg.alaska.gov

DGGS publications are also available at:

Alaska State Library, Historical
Collections & Talking Book Center
395 Whittier Street
Juneau, Alaska 99801

Alaska Resource Library and
Information Services (ARLIS)
3150 C Street, Suite 100
Anchorage, Alaska 99503

Suggested citation:

Wikstrom Jones, K.M., Wolken, G.J., and Daanen, R.P., 2026, Lidar-derived elevation data for upper Barry Arm fjord, southcentral Alaska, collected October 14, 2022: Alaska Division of Geological & Geophysical Surveys Raw Data File 2026-10, 10 p. <https://doi.org/10.14509/32063>



LIDAR-DERIVED ELEVATION DATA FOR UPPER BARRY ARM FJORD, SOUTHCENTRAL ALASKA, COLLECTED OCTOBER 14, 2022

Katreen M. Wikstrom Jones¹, Gabriel J. Wolken¹, and Ronald P. Daanen^{1*}

INTRODUCTION

The Alaska Division of Geological & Geophysical Surveys (DGGS) used aerial lidar to produce a classified point cloud, digital terrain model (DTM), surface model (DSM), and intensity model for Upper Barry Arm fjord with focus on the Barry Arm landslide, northeast of Whittier in Prince William Sound, southcentral Alaska, during near snow-free ground conditions. The goal of the survey is to provide snow-free surface elevation data to assess landslide movement using repeat surveys during snow-free conditions. Ground control was collected on July 27, 2022, and airborne data were collected on October 14, 2022, and subsequently processed in Terrasolid and ArcGIS. These data are provided as a Raw Data File under an open end-user license and are available on the DGGS website (<https://doi.org/10.14509/32063>).

LIST OF DELIVERABLES

- Classified Points
- DSM, DTM, and hydro-enforced DTM
- Intensity Image
- Metadata

MISSION PLAN

Aerial Lidar Survey Details

DGGS used a Riegl VUX1-LR laser scanner with a global navigation satellite system (GNSS) and a Northrop Grumman LN-200C inertial measurement unit (IMU) integrated by Phoenix LiDAR Systems. The sensor can collect a maximum of 820,000 points per second at a range of 215 m, or a minimum of 50,000 points per second at 820 m (ranges assume ≥ 20 percent natural reflectance). This survey was conducted with a pulse refresh rate of 400,000 pulses per second and a scan rate of 160 lines per second. We used a Cessna 180 Skywagon fixed-wing platform to survey from an elevation of approximately 100–300 m above ground level, at a ground speed of approximately 40 m/s, and with a scan angle set from 80 to 280 degrees. The total survey area was approximately 8.5 km² and excludes glaciers and water bodies, which lie *outside* the orange-outlined area of interest shown in the cover figure.

Weather Conditions and Flight Times

We flew the aerial survey on October 14, 2022, and covered three separate survey areas (Twentymile River, Barry Arm landslide, and Serpentine Glacier) between take-off and landing. The crew departed the Girdwood Airport at approximately 9:30 am and flew the Barry Arm landslide portion from 10:57 am to 11:42 am (fig. 1). The return flight landed back at Girdwood

¹Alaska Division of Geological & Geophysical Surveys, 3354 College Road, Fairbanks, AK 99709

*Former DGGS, in memoriam

Airport at approximately 1 pm. The weather throughout the survey was overcast with a high ceiling.

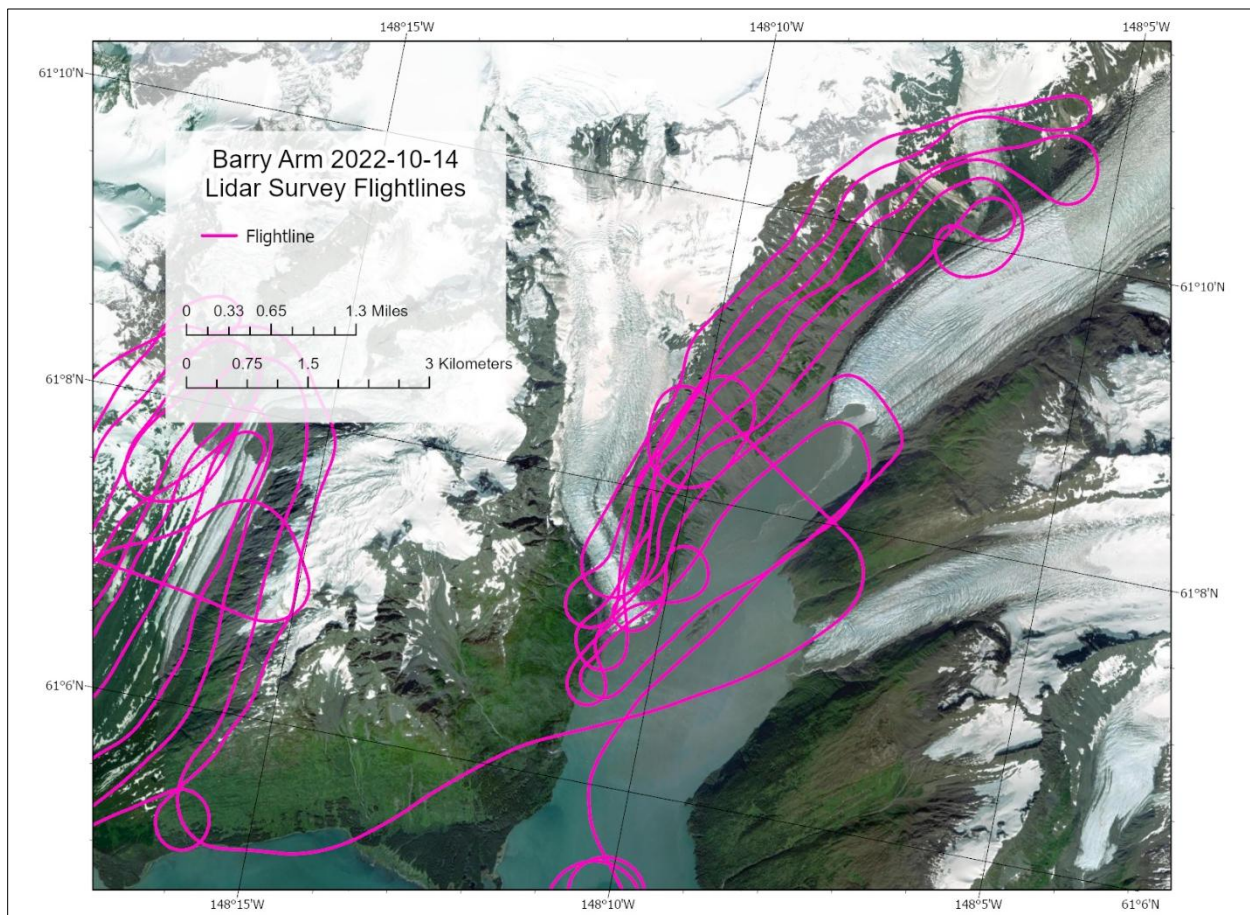


Figure 1. Lidar data collection flightlines.

PROCESSING REPORT

Lidar Dataset Processing

We processed point data in SDCimport for initial filtering and multiple-time-around (MTA) disambiguation. MTA errors corrected in this process stem from ambiguous interpretations of received pulse time intervals and occur more frequently at higher pulse refresh rates. IMU and GNSS data were processed in Inertial Explorer, and flightline information was integrated with the point cloud in Spatial Explorer. We calibrated the point data at an incrementally precise scale of sensor movement and behavior, incorporating sensor velocity, roll, pitch, and yaw fluctuations throughout the survey. For the lidar data collection, the pulse density is 28.9 pulses/m², and the average pulse spacing is 18.6 cm.

We created a macro (an ordered list of point classification commands tailored to this dataset) in Terrasolid software and classified points in accordance with the American Society for Photogrammetry & Remote Sensing (ASPRS) 2025 guidelines (ASPRS, 2025). After classification,

we applied a geometric transformation to convert points from ellipsoidal heights to GEOID12B (Alaska) orthometric heights.

Raster products were derived from the point cloud in ArcGIS Pro. A 50-cm DSM was interpolated from maximum elevation values in ground and vegetation classes using a triangulation method. A 50-cm DTM was interpolated from all ground-class returns using a triangulation method and minimum elevation values. We also produced a 1-m intensity image for the area using average binning in ArcGIS Pro, with no normalization or corrections applied. Water bodies and glacier surfaces were erased from the derived raster products.

Classified Point Cloud

Classified point cloud data are provided in LAZ format. Data are classified according to the ASPRS 2025 guidelines (table 1) and include return and intensity information. For classified ground points, the average point density is 13.4 pts/m², and the average spacing is 27.3 cm (fig. 2).

Table 1. Point cloud class code definitions.

Class Code	Description
1	Unclassified
2	Ground
3	Low Vegetation, $\geq 0.0\text{m}$, $< 0.5\text{m}$
4	Medium Vegetation, $\geq 0.5\text{m}$, $< 3\text{m}$
5	High Vegetation, $\geq 3\text{m}$
7	Low Noise
18	High Noise

Digital Surface Model

The DSM represents surface elevations, including the heights of vegetation, buildings, power lines, pipes, bridge decks, etc. The overall DSM is a single-band, 32-bit GeoTIFF file of 50 cm resolution. No Data value is set to $-3.40282306074\text{e}+38$ (32-bit, floating-point minimum).

Digital Terrain Model

The DTM represents bare earth elevations, excluding vegetation, bridge decks, buildings, etc. The overall DTM is a single-band, 32-bit GeoTIFF file of 50 cm resolution. The No Data value is set to $-3.40282306074\text{e}+38$.

Lidar Intensity Image

The lidar intensity image describes the relative amplitude of reflected signals contributing to the point cloud. Lidar intensity is (1) primarily a function of scanned object reflectance in relation to the signal frequency, (2) dependent on ambient conditions, and (3) not necessarily consistent between separate scans. The intensity image is a single-band, 32-bit GeoTIFF file of 1 m resolution. No Data value is set to $-3.40282306074\text{e}+38$.

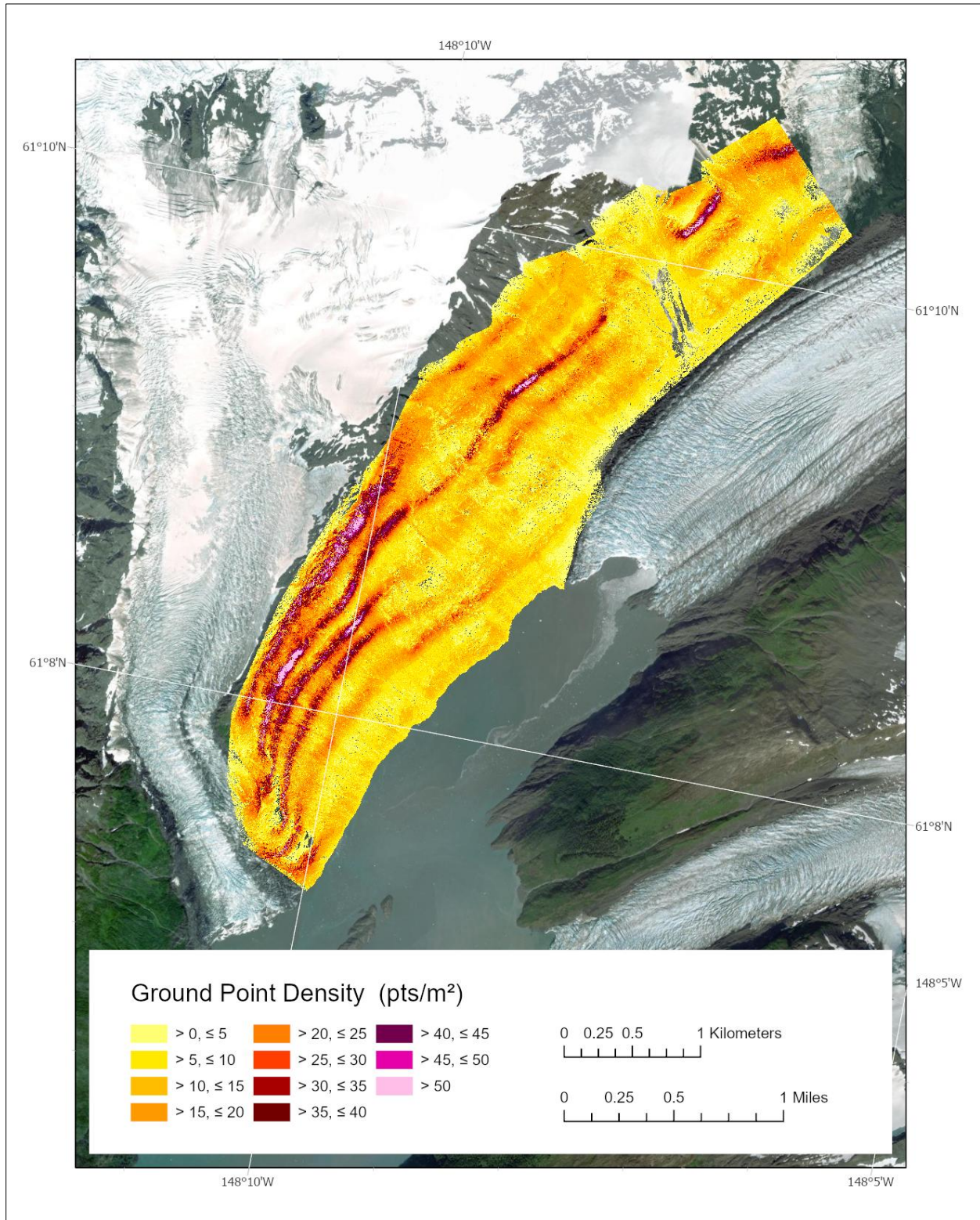


Figure 2. Ground point density for the survey displayed as a raster.

SURVEY REPORT

Ground Survey Details

Ground control and checkpoints were collected on July 27, 2022. A Trimble R10-2 GNSS receiver with an internal antenna was deployed at the southern tip of the island below the landslide (see cover figure). It provided a base station occupation and real-time kinematic (RTK) corrections to points surveyed with a rover Trimble R10-2 GNSS receiver (internal antenna). We collected 73 ground control and checkpoints across the survey area for calibration and to assess the vertical accuracy of point clouds generated from multiple repeat Barry Arm surveys. Sixty-Six of these were used for this lidar acquisition; the remainder were excluded due to insufficient point-cloud overlap. Checkpoints were collected on bare earth or minimally vegetated surface.

Coordinate System and Datum

We processed and delivered all data in NAD83 (2011), UTM6N, and vertical datum NAVD88 GEOID12B.

Horizontal Accuracy

Horizontal accuracy was not measured for this collection; it is considered inherent in the airborne GPS/IMU solution.

Vertical Accuracy

We measured a vertical mean offset of +8.1 cm between 52 control points and the point cloud (app. 1). This offset was reduced to -1.5 cm by applying a constant vertical correction to the lidar point data. We used 14 checkpoints to determine the non-vegetated vertical accuracy (NVA) of the point cloud ground class, using a triangulation-based approach. Project NVA was calculated to have a root mean square error (RMSE) of 5 cm (app. 2). Relative accuracy was evaluated based on interswath overlap consistency, yielding an RMSE of 0.8 cm.

Data Consistency and Completeness

This is a full-release dataset. There was no over-collect. Data quality is consistent throughout the survey, save for gaps over bodies of water, glaciers, and snow-covered surfaces.

ACKNOWLEDGMENTS

These data products were funded by the U.S. Geological Survey Cooperative Agreement Grant #G21AC10362 and collected and processed by DGGS. The views and conclusions contained in this document are those of the authors and should not be interpreted as representing the opinions or policies of the USGS. Mention of trade names or commercial products does not constitute their endorsement by the USGS. We thank Clearwater Air and Alpine Air for their aviation expertise and contribution to these data products.

REFERENCES

The American Society for Photogrammetry & Remote Sensing (ASPRS), 2025, LAS Specification 1.4 - R16. <https://publicdocuments.asprs.org/las-v14-r16-2025>

APPENDIX 1: GROUND CONTROL POINTS

GCP	Easting (m)	Northing (m)	Known Z (m)	Laser Z (m)	Dz (m)
1	437488.493	6776454.695	8.111	8.21	0.099
2	437487.745	6776455.47	8.061	8.16	0.099
3	437492.552	6776458.051	9.615	9.73	0.115
4	437501.304	6776462.046	9.864	9.96	0.096
5	437502.207	6776459.714	9.394	9.49	0.096
6	437509.001	6776468.295	10.88	10.97	0.09
7	437504.688	6776476.88	8.942	9.04	0.098
8	437508.148	6776482.664	10.694	10.78	0.086
9	437508.785	6776483.122	10.679	10.75	0.071
10	437511.669	6776482.462	10.549	10.63	0.081
11	437514.356	6776505.024	12.711	12.81	0.099
12	437508.704	6776500.934	11.63	11.71	0.08
13	437509.065	6776502.382	11.795	11.9	0.105
14	437504.077	6776509.524	13.486	13.56	0.074
15	437503.374	6776513.125	13.389	13.48	0.091
16	437502.934	6776520.358	12.676	12.8	0.124
17	437495.714	6776508.843	15.289	15.38	0.091
18	437493.835	6776507.75	15.172	15.27	0.098
19	437494.038	6776505.654	15.069	15.16	0.091
20	437492.722	6776506.163	15.118	15.22	0.102
21	437492.149	6776506.37	15.119	15.21	0.091
22	437492.92	6776505.685	15.086	15.19	0.104
23	437489.165	6776502.981	14.638	14.74	0.102
24	437480.281	6776497.017	12.852	12.93	0.078
25	436881.293	6779651.902	1082.028	1082.18	0.152
26	436881.574	6779613.272	1077.565	1077.61	0.045
27	436878.023	6779559.375	1083.938	1084.09	0.152
28	436878.672	6779555.834	1084.665	1084.83	0.165
29	436877.302	6779552.042	1084.511	1084.6	0.089
30	436876.834	6779550.482	1084.467	1084.58	0.113
31	436884.149	6779519.775	1082.734	1082.88	0.146
32	436876.001	6779506.761	1081.73	1081.8	0.07
33	436876.348	6779506.377	1081.644	1081.7	0.056
34	436864.716	6779493.197	1077.129	1077.14	0.011
35	436925.503	6779599.375	1071.038	1071.03	-0.008
36	436939.101	6779586.8	1070.056	1070.15	0.094
37	438464.148	6777743.439	10.243	10.23	-0.013
38	438463.458	6777738.12	9.69	9.76	0.07
39	438454.754	6777734.505	8.231	8.31	0.079
40	438438.33	6777720.901	8.98	9.04	0.06

41	438436.914	6777719.49	8.951	8.99	0.039
42	438429.634	6777698.593	5.698	5.74	0.042
43	438429.075	6777697.524	5.713	5.76	0.047
44	438413.618	6777690.325	5.147	5.22	0.073
45	438412.196	6777685.616	3.989	4.03	0.041
46	438399.845	6777676.952	4.128	4.17	0.042
47	438402.825	6777676.655	4.121	4.1	-0.021
48	438395.896	6777686.643	6.075	6.16	0.085
49	438392.303	6777688.523	5.636	5.7	0.064
50	438386.864	6777676.49	6.756	6.85	0.094
51	438382.106	6777671.618	5.58	5.66	0.08
52	437519.303	6776477.394	9.792	9.88	0.088
Average dz (m)	0.081				
Minimum dz (m)	-0.021				
Maximum dz (m)	0.165				
Average magnitude error (m)	0.083				
Root mean square error (m)	0.089				
Standard deviation (m)	0.038				

APPENDIX 2: CHECKPOINTS

Check point	Easting (m)	Northing (m)	Known Z (m)	Laser Z (m)	Dz (m)
1	437507.9	6776467.6	10.728	10.76	0.032
2	437497.5	6776462.6	10.304	10.31	0.006
3	437506	6776481.2	10.576	10.6	0.024
4	437514.2	6776504.2	12.732	12.76	0.028
5	437502.9	6776515	13.338	13.33	-0.008
6	437493.4	6776505.9	15.097	15.13	0.033
7	437481.1	6776499.9	12.826	12.81	-0.016
8	436884.7	6779603.5	1078.149	1078.05	-0.099
9	436881.6	6779534.4	1082.655	1082.66	0.005
10	436914	6779612.9	1072.23	1072.25	0.02
11	438465.2	6777739.3	10.175	10.05	-0.125
12	438428.3	6777706.5	7.549	7.49	-0.059
13	438408.4	6777683.2	4.091	4.05	-0.041
14	438391	6777680.3	6.496	6.49	-0.006
Average dz (m)	-0.015				
Minimum dz (m)	-0.125				
Maximum dz (m)	0.033				
Average magnitude error (m)	0.036				
Root mean square error (m)	0.05				
Standard deviation (m)	0.049				



In Memoriam
Ronald P. Daanen